PRAMANA
— journal of
physics

Vol. 74, No. 2
February 2010
pp. 231–246

Search for invisibly decaying Higgs boson at Large Hadron Collider

S BANSAL[1], K MAZUMDAR[2,*] and J B SINGH[1]
[1]Department of Physics, Panjab University, Chandigarh 160 014, India
[2]Tata Institute of Fundamental Research, Homi Bhabha Road, Mumbai 400 005, India
[*]Corresponding author. E-mail: mazumdar@mailhost.tifr.res.in

MS received 23 March 2009; revised 28 August 2009; accepted 15 September 2009

Abstract. In several scenarios of Beyond Standard Model physics, the invisible decay mode of the Higgs boson is an interesting possibility. The search strategy for an invisible Higgs boson at the Large Hadron Collider (LHC), using weak boson fusion process, has been studied in detail, by taking into account all possible backgrounds. Realistic simulations have been used in the context of CMS experiment to devise a set of event selection criteria which eventually enhances the signal contribution compared to the background processes in characteristic distributions. In cut-based analysis, multi-jet background is found to overwhelm the signal in the finally selected sample. With an integrated luminosity of 10 fb^{-1}, an upper limit of 36% on the branching ratio can be obtained for Higgs boson with a mass of 120 GeV/c^2 for LHC energy of 14 TeV. Since the analysis essentially depends on the background estimation, detailed studies have been done to determine the background rates from real data.

Keywords. Invisible Higgs; compact muon solenoid detector.

PACS No. 13.90.+i

1. Introduction

The electroweak symmetry breaking (EWSB) by Higgs mechanism is yet to be tested experimentally which demands the observation of the Higgs boson. Thus the only missing block of the otherwise tremendously successful Standard Model (SM) is the lack of confirmation of the Higgs sector and hence the discovery of the Higgs boson is very crucial for high energy physics. Subsequent to the discovery, a detailed study of the properties of the Higgs boson at the Large Hadron Collider (LHC) is equally important to establish the nature of the particle. The branching ratios of various decay modes are essential to determine the Higgs couplings to the vector bosons as well as the fermions. Needless to say that it is also very important to search for all possible decay modes, as part of the programme, to investigate the properties of the Higgs boson in detail. In particular, observation of invisible

decay mode of Higgs boson will immediately signify the presence of New Physics beyond SM.

In SM, the Higgs boson can be produced by several processes at hadron colliders, among which gluon–gluon fusion has the highest rate followed by the weak boson fusion (WBF) mechanism at the LHC. The associated production modes, where the Higgs boson is accompanied by a W or Z boson or by a pair of heavy quarks in the final state, have much lower rates.

Most of the Higgs search analyses assume that the Higgs boson will predominantly decay into detectable particles. However, in Beyond Standard Model (BSM) scenarios, this assumption may not be correct if there are new, weakly interacting particles, which couple to the Higgs boson with enough strengths. If these weakly interacting particles are neutral and stable, the Higgs boson will decay invisibly. There are many models in which this situation is realized, like, when the Higgs boson decays to a pair of majorons [1]. In general, in models of dark matter with a stable singlet scalar, the Higgs boson can decay invisibly. In several scenarios, such as models of 4th generation neutrino [2], the branching fraction to the invisible decay mode is dominant in the low-mass range before the decay mode of the Higgs boson to the pair of vector bosons opens up. This is particularly significant, because of the present indication of a reasonably low-mass Higgs boson in SM.

In models of large extra dimensions, the Higgs boson can mix with graviscalar which escapes the detector [3]. It is also possible that the Higgs boson decays to Kaluza–Klein neutrinos [4], which are allowed to propagate in the bulk. If the Higgs boson mass is less than about 160 GeV/c^2, the decay width to the SM particles is quite low. But in such a case, the invisible decay width can be significantly large. In supersymmetric models, the Higgs boson can decay into a pair of lightest neutralinos when the unification constraint at the GUT scale is removed [5].

Experimental discovery of an invisible Higgs boson does not entail reconstruction of the mass peak, rather, it requires a significant excess in the number of observed events over the expected number from all background processes in characteristic distributions. The exercise described here for the determination of the significance for excess is model-independent and thus can be used for interpretation of any model of invisible Higgs boson. In this study, the invisible Higgs boson is assumed to be produced with SM production rate and an invisible branching fraction of 100% have been assumed. Consequently, the results can be scaled for a non-SM Higgs boson production rate multiplied by a fractional decay branching. Thus, the signal rate S is scaled by the production rate and the invisible branching fraction $\mathrm{BR_{inv}}$:

$$S = S_0 \frac{\sigma}{\sigma_{\mathrm{SM}}} \frac{\mathrm{BR_{inv}}}{1},$$

where S_0 is the signal rate obtained from the studies, $\sigma/\sigma_{\mathrm{SM}}$ is the ratio of the non-standard production cross-section to that of the SM production and $\mathrm{BR_{inv}}$ is the invisible decay branching fraction.

The LEP experiment has searched for the invisible decay mode of the Higgs boson assuming SM production of Bjorken process. With 95% CL, a lower bound of 114.4 GeV/c^2 has been assumed on the mass of Higgs boson [6]. At Tevatron, no experimental analysis of invisible decay mode of the Higgs boson is reported. However, phenomenological studies envisage that 5σ discovery is possible for the

Higgs boson of mass 120 GeV/c^2 with a luminosity of 30 fb^{-1} [7]. It may also be possible at Tevatron to combine the associated production mode and WBF mode to search for the invisible Higgs boson with less than 10 fb^{-1} at 3σ level [8].

We report a search strategy using WBF mode in the context of LHC operation at 14 TeV. We have estimated the reach in branching fraction as a function of the mass of the Higgs boson as well as the accumulated luminosity.

2. Compact muon solenoid (CMS) detector

The present analysis has been done using compact muon solenoid (CMS) detector configuration, one of the two general purpose experiments at the LHC. The main parts of the detector are tracker, electromagnetic calorimeter (ECAL), hadronic calorimeter (HCAL) and muon chambers, positioned radially outwards from the beam–beam collision point providing excellent resolutions for the measurement of position, momentum and energy of muons, electron and photons [9]. Figure 1 provides a three-dimensional overview of the CMS detector along with its dimensions. The tracker is designed for high-resolution momentum measurement of charged particles and vertex reconstruction in the range $|\eta| < 2.4$. The ECAL is designed for detection and energy measurement of electromagnetic particles up to $|\eta| < 3$. The HCAL is meant for detection and energy measurement of hadronic particles and up to $|\eta| < 5$ providing the hermiticity of the detector, specially for missing

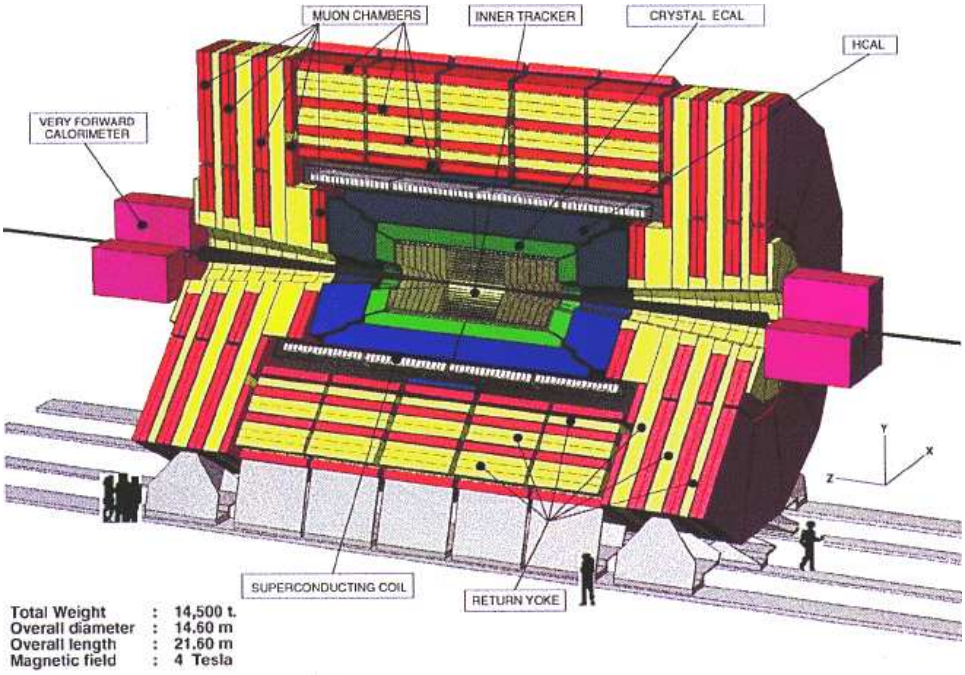

Figure 1. Three-dimensional overview of the CMS detector.

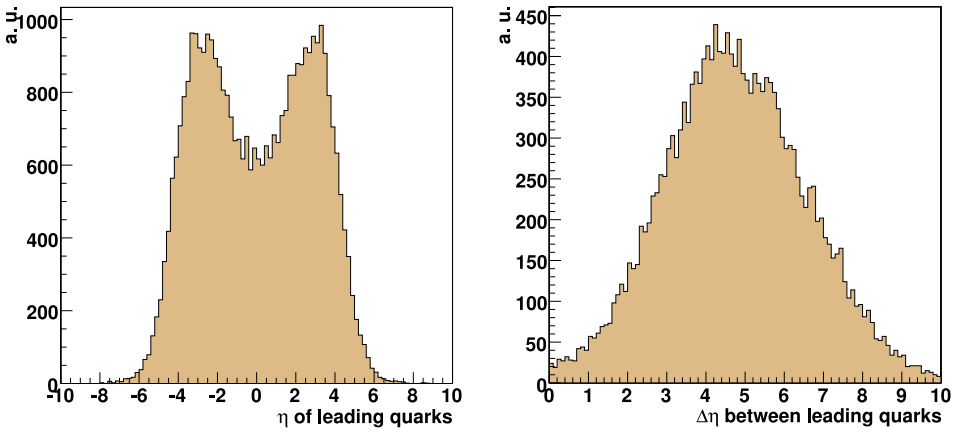

Figure 2. Pseudorapidity (η) distribution of leading quarks (left) and $\Delta\eta$ between leading quarks (right) for signal events.

energy measurements. The outermost subdetector is the muon-chambers system which identifies and measures muons accurately.

3. Invisible Higgs signal characteristics in WBF process

Since the Higgs boson decays invisibly, the detection of the event at LHC, where predominantly the Higgs boson is singly produced, is difficult as it has to be then based only on missing energy in the transverse direction to the beam. To identify the invisibly decaying Higgs boson event, processes with additional particles in the final state have to be utilized. For this purpose, the weak boson fusion (WBF) process, $qq \to qqH$, is the best suited, since the topological properties of the events can be conveniently utilized to control backgrounds as pointed out in [10].

The initial state quarks, after emitting a weak vector boson each (both have to be either W or Z), mostly tend to continue in the original directions resulting in two jets with large (pseudo) rapidity (η) gap as shown in figure 2. The leading quarks have moderate transverse momentum but they carry large amount of energies, resulting in large dijet invariant mass as depicted in figure 3 (left). Further, the quarks are in opposite hemispheres and they do not have any colour-connection with each other coming from opposite beams. Additionally, since the Higgs boson is decaying invisibly, there is not much hadronic activity in the intermediate region between the quarks. Interestingly, the leading quarks get balanced by the Higgs boson resulting in an angle in the transverse plane smaller than π between these quarks as shown in figure 3 (right). The signal events, of course, have reasonably large amount of missing energy, the transverse component of which can be detected only in the experiment, referred to as $\not{E}_{\mathrm{T}}$. Based on these characteristics, a set of requirements to select events for enhancing signal to background ratio has been proposed as WBF selections in [10] and we have mostly followed the recipe in addition to complementing the selection with additional considerations.

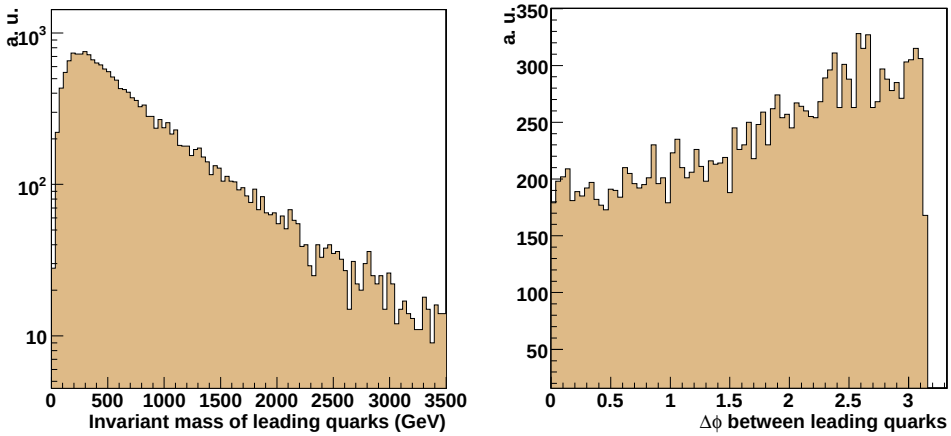

Figure 3. Invariant mass of leading quarks (left) and $\Delta\Phi$ between leading quarks (right) for signal events.

4. Backgrounds and the event simulation

In this study, all the major SM processes, which can potentially pose as backgrounds to invisible Higgs boson mode, have been considered.

- Inclusive W + jet process, with $W \to \ell\nu$, $\ell = e$, μ and τ, where the charged lepton is not identified in the detector and the two jets satisfy WBF conditions.
- Inclusive Z + jet process, with $Z \to \nu\nu$ and the two jets satisfy WBF conditions.
- QCD multijet events where the two leading jets satisfy WBF conditions and $\not\!\!E_{\mathrm{T}}$ is mostly due to the detector imperfections and limited acceptance of jets. Additionally, a genuine contribution to the $\not\!\!E_{\mathrm{T}}$ may also be due to the semileptonic decays of heavy quarks produced in the hadronic interactions.
- Inclusive $t\bar{t}$ production process which has large production rate at LHC, may mimic the signal characteristics, though with small probability. Hence we did investigate this process.

PYTHIA Monte Carlo generator package [11] has been used for generating signal and QCD multijet events. Inclusive W/Z + jet events were generated using ALPGEN package [12], whereas MC@NLO [13] has been used for inclusive $t\bar{t}$ events generation. Since the multijet events have very large cross-sections, $\mathcal{O}(\mu b)$ in total, to have enough statistics for events with high inelasticity, event samples were split into multiple contiguous $\hat{p}_{\mathrm{T}}$-bins: 20–30, 30–50, 50–70, 70–100, 100–150, 150–250, 250–400, 400–1200 GeV/c. Here $\hat{p}_{\mathrm{T}}$ parameter corresponds to the minimum transverse momentum of the final-state partons in the $2 \to 2$ hard interaction subprocess and hence related to the usual Q^2 value. This helped one to understand the nature of QCD background contribution better and hence to devise and optimize event selection criteria to tackle it.

Potentially, the New Physics causing the invisible decay of the Higgs boson may also give rise to other processes, consistent within the same model, which may mimic the signal signatures. But other than supersymmetry (SUSY), no other BSM scenario has complete kinematic prescription for such possibilities. With current experimental bounds on the squark and gluino masses, for potential SUSY events, the final states are likely to have busy event topology due to the heavy masses involved. The signal event with only two forward and backward jets are in strong contrast with those. Hence, the survival rate of SUSY processes to pass all our selection criteria, as discussed below, is negligible.

Since the measurement of the jet and $\not{E}_{\mathrm{T}}$ are crucially dependent on the detector, a full-fledged simulation of the detector effects is essential for a realistic evaluation of the physics potential. It is to be noted that this is the first detailed study of all the background processes which can mimic the signal. The events from various generator packages were passed through detailed GEANT4 simulation of the CMS detector and reconstruction chains to produce samples as realistic as possible to the actual data expected in the experiment.

5. Reconstruction and selection of events

Jets are reconstructed with iterative cone algorithm of cone radius $\Delta R = \sqrt{\Delta\eta^2 + \Delta\Phi^2} = 0.5$ in $\eta \times \Phi$ space [14] and the measured energy is corrected for η and p_{T} dependance [15]. The $\not{E}_{\mathrm{T}}$ in the event is determined using calorimeter towers only and then calibrated by the method described in [16].

Electrons and muons reconstructed using CMS standard methods as described in [17] and [18], are required to be isolated from the neighbouring energetic tracks. For electrons, the track isolation is defined as $\sum(p_{\mathrm{T}}^{\mathrm{track}}/p_{\mathrm{T}}^{\mathrm{ele}})^2 \leq 0.02$, where the sum runs over all tracks, with $(p_{\mathrm{T}})^{\mathrm{track}} \geq 1.5$ GeV/c, within an $\eta \times \Phi$ annular isolation cone centred on the reconstructed electron between $0.02 < \Delta R < 0.6$. The sum excludes the candidate electron which has a transverse momentum of $p_{\mathrm{T}}^{\mathrm{ele}}$ [19]. For muons, the tracker isolation is defined as $\sum p_{\mathrm{T}} \leq 3$ GeV/c, where again all the tracks, other than the muon candidate, within the cone of $\Delta R = 0.3$ have been considered [20].

The events are considered to be triggered (or recorded permanently for off-line future analyses) by the on-line measurements. The selected events are required to have at least two identified jets and $\not{E}_{\mathrm{T}}$ should be greater than 60 GeV. The jets should have transverse momentum $p_{\mathrm{T}}^{1,2} > 40$ GeV/c, in opposite hemispheres ($\eta_1 \times \eta_2 < 0$) and large rapidity gap ($\Delta\eta_{12} > 4.4$) [21]. The trigger efficiency for signal events in the mass range 120–140 GeV/c^2 is about 18% whereas that of W/Z + jet events it is about 3–5% and for inclusive top-pair production events it is much lower (about 0.6%). The two leading jets in the event are referred to as tagging jets.

Subsequently, for off-line analysis, the invariant mass of the tagging jets is required to be more than 1200 GeV/c^2. The triggering characteristics and the di-jet mass criteria are collectively referred to as WBF condition since they are meant to enhance the signal contribution compared to background processes in the selected sample. Since no leptonic production is expected in the signal process, an event is

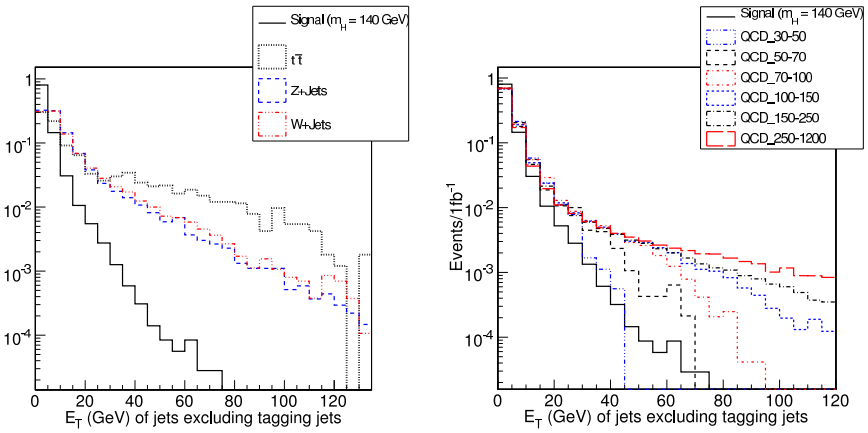

Figure 4. Uncorrected transverse energy of additional jet in between tagging jets ($\eta^{j\min} + 0.5$, $\eta^{j\max} - 0.5$). Left plot is for Z/W + jets and $t\bar{t}$ events and right plot is for QCD events.

rejected if it contains an isolated electron with $p_T > 10$ GeV/c and $|\eta| < 2.4$ or a muon with $p_T > 5$ GeV/c and $|\eta| < 2.1$.

Events are further selected by applying a harder cut on $\not{E}_T$ compared to that at trigger level; the corrected $\not{E}_T$ in the event is required to be above 100 GeV. High energy QCD multijets events, which are also likely to produce larger amount of $\not{E}_T$ in the detector, are tackled subsequently using other discriminating characteristics of the signal events.

Applying a veto on any additional hadronic activity between tagging jets is aimed to reduce all background channels substantially while keeping a high signal efficiency. The presence of additional hadronic activity in the pseudorapidity region between the tagging jets for signal and background events are shown in figure 4. Background reduction is achieved to a good extent by applying central jet veto (CJV) condition whereby an event with a third jet is rejected if it has a transverse energy greater than 15 GeV and if it is located in the region defined by $\eta^{j\min} + 0.5 < \eta^{j3} < \eta^{j\max} - 0.5$ where $\eta^{j\min}$ and $\eta^{j\max}$ refer to the pseudorapidities of the tagging jets and η^{j3} corresponds to the third jet.

To suppress mainly the QCD multijet background up to a satisfactory level, additionally a jet energy-based criteria is used based on the variable:

$$\mathrm{NV} = \frac{(E_T^{\mathrm{miss}})^2 - (E_T^{j1} - E_T^{j2})^2}{(E_T^{j2})^2}.$$

The distribution of NV variable for QCD and the signal events is shown in figure 5. Ideally, NV will be zero for QCD di-jet events and positive for events which have real missing energy as in our case of signal events. However, because of the hard gluon radiations produced in the fragmentation of the primary partons, the jet algorithm may reconstruct additional jets depending on the broadness of the partonic jet, thus affecting the naive picture of the NV variable. Depending on how partonic jets are affected, the difference between the two most energetic jets will

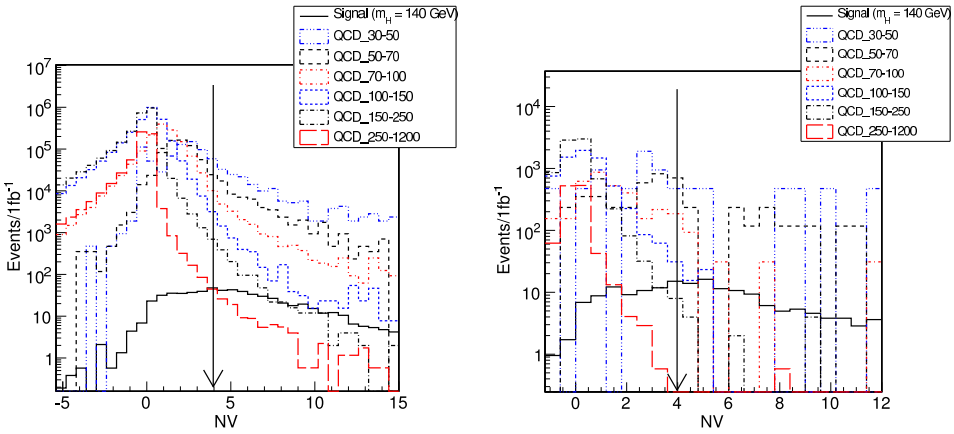

Figure 5. NV distribution for signal and various QCD bins for events with two jets in opposite hemispheres (left plot) and after WBF, $\not\!\!E_{\rm T} \geq 100$ GeV, CJV cut (right plot).

Table 1. Estimated cross-section (in fb) for signal and backgrounds (W + jets, Z + jets and inclusive $t\bar{t}$ processes) for successive selection criteria.

Sample	Signal ($m_{\rm H}$ = 140 GeV/c^2)	Z + jets	W + jets	Inclusive $t\bar{t}$
HLT Condition	673	3800	12680	4870
Lepton veto	660	3717	8388	2449
WBF	286	911	2255	898
$\not\!\!E_{\rm T} > 100$ GeV	241	631	1117	355
CJV	190	216	289	38
NV > 4	119	92	95	7
$\Delta\Phi_{jj} < 1.5$ rad	101	64	79	5

vary. If hard gluon radiation is predominant in one of the jets, $E_{\rm T}^{j1} - E_{\rm T}^{j2}$ will be large. On the other hand, since $\not\!\!E_{\rm T}$ is measured by taking into account the energy deposits in all calorimeter towers, it is less sensitive to this effect which leads to a negative NV value. In this analysis, events are required to have NV value more than 4.

For most of the background events, the jets are back-to-back in the transverse plane as opposed to the signal events where the jets are closer to balance the massive Higgs boson. This feature is manifest in the angular correlation between the tagging jets as given by $\Delta\Phi_{jj}$ variable. Figure 6 displays the distributions for signal and background events after the requirements of lepton veto, WBF condition, $\not\!\!E_{\rm T}$ requirements and CJV conditions. Finally events are selected in the range $\Delta\Phi_{jj} \leq 1.5$ radians.

The cross-section, in units of fb ($=10^{-39}$ cm^2), after each selection step, for invisible Higgs boson signal in WBF process, Z + jets, W + jets and $t\bar{t}$ + jets are shown in table 1 and that for QCD multijet background in table 2.

Table 2. Estimated cross-section (in fb) for signal and QCD multijet background in various $\hat{p}_T$-bins for successive selection criteria.

Sample	QCD (20–30)	QCD (30–50)	QCD (50–70)	QCD (70–100)	QCD (100–150)	QCD (150–250)	QCD (250–400)	QCD (400–1200)
Scale factor	1129	476	118	20.8	7.76	1.99	0.58	0.35
$\sigma\times$Filter eff. (fb)	1197560	1045200	891800	1582680	3105000	2662500	545400	96230
Lepton veto	1193030	1038156	884646	1564520	3072708	2630640	537546	94527
WBF	46408	98056	142308	318941	625911	352694	27200	1446
$\not{E}_T > 100$ GeV	15847	33320	22302	29016	34544	34562	5383	310
CJV	4528	9520	5782	3648	7634	8767	1205	43
NV > 4	3395	4760	2478	341	54	10	1	1
$\Delta\Phi_{jj} < 1.5$ rad	3395	476	1770	155	45	8	0	0

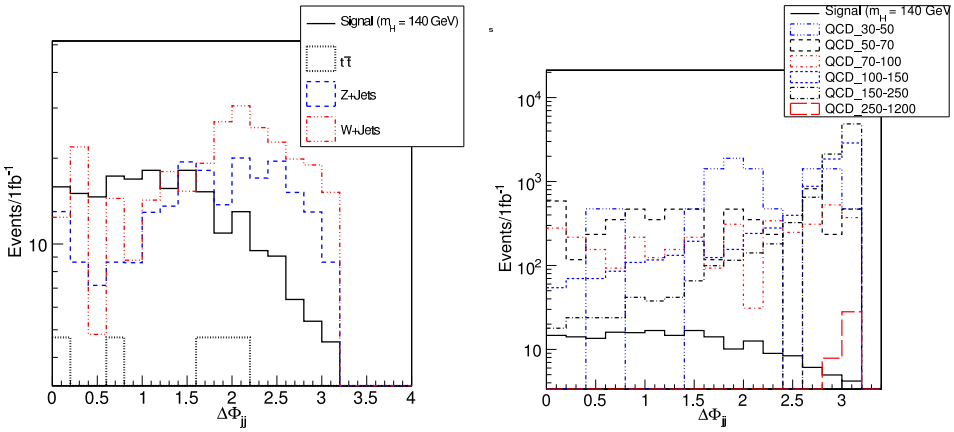

Figure 6. $\Delta\Phi_{jj}$ between leading jets after lepton veto, WBF conditions, $\not{E}_T$ and CJV requirements. The left plot is for W + jets, Z + jets and inclusive $t\bar{t}$ events while the right plot is for QCD multijet events.

6. Signal significance

The signal significance is calculated using the final numbers of selected samples for signal and background processes as given in tables 1 and 2. For 1 fb^{-1} of accumulated luminosity, the total number of background events in the selected sample is about 5997 and the number of signal events for a Higgs boson of mass 120 GeV/c^2 is 109 leading to a statistical significance of the signal, $S/\sqrt{B}$ value, to be equal to 1.41.

However, in this analysis, performance of the calorimeter which measures the jets is very crucial and correspondingly there are significant systematics involved. We have estimated the uncertainty in the estimated number of signal events due to two sources: jet-energy-scale and the scale for $\not{E}_T$. The conservative estimate of the total uncertainty is about 15%. The systematics will be more accurately determined for the background events, and we have assumed 5% total uncertainty in background estimation which is anticipated to be mostly due to luminosity measurements.

Table 3. The signal significance for different values of the Higgs boson mass. The total number of background events is estimated to be about 6000.

Signal Higgs boson mass (GeV/c^2)	120	140	160
Cross-sction (fb)	4470	3830	3320
Trigger efficiency (%)	16.27	17.57	18.65
Off-line selection efficiency (%)	15.30	14.99	14.42
Cross-section after all selections (fb)	109	101	89
$S/\sqrt{B}$	1.41	1.30	1.15
Signal significance ($Scp = Sc12$)	0.38	0.35	0.31

The above uncertainties are taken into account to estimate the experimental significance. The signal being overwhelmed by the background, we quote a parameter used in experimental analysis which is equivalent to the p-value of a result. The significance Scp is the probability from Poisson distribution with means as the background event number b to observe a total of at least $b + s$ number of background and signal events, converted to the equivalent number of standard deviations of a Gaussian distribution [22].

$$\beta = \int_{Scp}^{\infty} \mathrm{e}^{-x^2/2}\mathrm{d}x, \quad \text{where } \beta = \sum_{i=s+b}^{\infty} \frac{b^i \mathrm{e}^{-b}}{i!}.$$

For the 95% CL upper limit, $\beta = 1.64$. In table 3 results for various Higgs boson mass values corresponding to an integrated luminosity of 1 fb^{-1} are presented.

7. Discovery potential

In order to estimate the potential of CMS experiment to discover an invisibly decaying Higgs boson, the best way is to provide the experimentally estimated number of signal events, in excess of backgrounds, which can be related to any scenario of BSM that envisages an invisibly decaying Higgs boson. In this regard a model-independent variable ξ^2 is defined as

$$\xi^2 = \mathrm{BR}_{\mathrm{inv}} \cdot \frac{\sigma_{\mathrm{BSM}}}{\sigma_{\mathrm{SM}}},$$

where the second term is a factor which takes into account the production rate of an invisible Higgs boson in any BSM scenario, scaled by the rate of WBF production process in SM, which is the default assumption in the analysis presented. Thus if $\sigma_{\mathrm{BSM}} = \sigma_{\mathrm{SM}}$, then ξ^2 is equivalent to the branching fraction $\mathrm{BR}_{\mathrm{inv}}$. The signal significance being quite poor with data corresponding to integrated luminosity of 1 fb^{-1}, no sensible value for ξ^2 could be obtained. Table 4 shows the maximum ξ^2 values which can be probed, at 95% CL, for two values of integrated luminosity, 10 fb^{-1} and 30 fb^{-1}, as a function of the Higgs boson mass. The dependence of ξ^2 parameter as a function of Higgs boson mass is shown in figure 7 for different values of integrated luminosity.

Table 4. The values of ξ^2 which can be probed for integrated luminosities of 10 fb^{-1} and 30 fb^{-1} as a function of Higgs boson mass.

m_{H} (GeV/c^2) $\rightarrow$	120	140	160
Integrated luminosity (fb $^{-1}$)$\downarrow$			
10	0.36	0.39	0.45
30	0.21	0.23	0.26

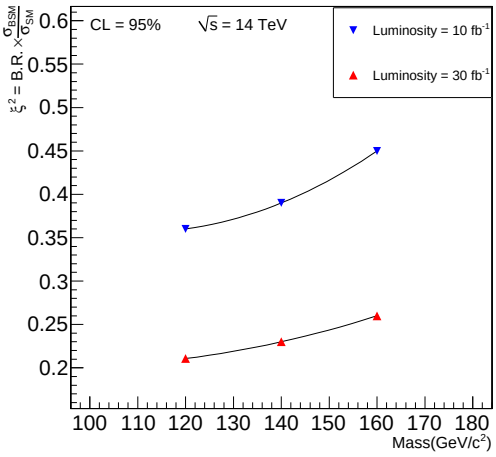

Figure 7. ξ^2 as function of Higgs mass (GeV/c^2) for different values of integrated luminosity.

It is very likely that due to different couplings, the production cross-section of an invisibly decaying Higgs boson will differ from that of SM cross-section. Assuming that the background is only due to SM processes, the signal significance can be determined as a function of the required luminosity having determined the ξ^2 value at a given luminosity using the formula:

$$\mathcal{L} = \mathcal{L}_0 \left[\frac{\sigma_{\mathrm{BSM}}}{\sigma_{\mathrm{SM}}} \frac{\mathrm{BR}_{\mathrm{inv}}}{1} \right]^{-2}.$$

Thus, assuming $\sigma_{\mathrm{BSM}} = \sigma_{\mathrm{SM}}$, we can calculate the minimum required integrated luminosity to obtain an upper limit on the branching ratio for invisible decay at 95% CL. Hence for $\mathrm{BR}_{\mathrm{inv}} = 50\%$ and for Higgs boson mass values of 120, 140 and 160 GeV/c^2, the luminosity values are 5.12 fb^{-1}, 6.1 fb^{-1} and 8.1 fb^{-1} respectively.

8. Methods for background estimation

We describe below briefly, the data-driven methods which can be adopted to estimate the background rates. During the early phase of LHC operation, all the SM processes, in particular the 'standard candles', like W and Z events were measured

accurately. With few tens of pb^{-1} of data, the rates of Z/W + n-jets background events ($n = 1, 2, 3, \ldots$) are expected to be determined accurately using $Z \to \ell\ell$ and $W \to \ell\nu$ modes, where $\ell = e, \mu, \tau$. It is to be noted that the production process and the anticipated hadronic activities in these W + jet events are similar to that in Z + jet events. Further, the branching ratios of Z and W to leptons are well measured. Effectively, after accounting for the branching ratios, the difference between the two processes is that of detector acceptance. Subsequently, the fraction of W/Z + jet events which are likely to pass the WBF criteria and other selections can be obtained accurately utilizing the leptonic modes.

For the QCD multijet events, the study is limited by the statistics of the simulated sample which will not be an issue with the real data. With an integrated luminosity of less than 1 fb^{-1}, the CMS experiment will be able to estimate the shape of $\not{E}_{\text{T}}$ distribution in multijet events quite well, assuming that the jet-energy scale as well as other calibrations are established by that time.

8.1 *Estimation of the rate of $Z \to \nu\nu$ + jet events using $W \to \mu\nu$ + jet events*

The rate of $Z \to \nu\nu$ + jet process can be estimated using the $W \to \mu\nu$ + jet events which contain a single, well-reconstructed, isolated muon with $p_{\text{T}} > 20$ GeV/c and $|\eta| < 2.1$. However, due to difference in the initial and final states, correction factors have both theoretical and experimental components.

- Events have to be corrected for limited detector acceptance (η coverage) and also for the threshold placed on the transverse momentum of the reconstructed muons, i.e., $|\eta| < 2.1$ and $p_{\text{T}} > 20$ GeV/c. It is estimated to be 48% using information at the event generation level.
- Muon isolation efficiency will be measured from the data using $Z \to \mu\mu$ events with a tag and a probe method whereby one of the muons is required to satisfy a stricter criteria (to be called tagging muon) than the other (called probe muon). Isolation efficiency using Monte Carlo reconstructed sample is estimated to be 90%.

Combination of these two effects yields a total efficiency of 42% which corresponds to an experimental correction factor of 2.38.

Theoretically, the production rates of W and Z are different due to different masses and different partons involved at the production vertex. Leptonic branching ratios also are different. Taking all these into account the correction factor amounts to 0.72.

Thus, the total correction factor is 1.714 which is the product of experimental and theoretical factors. After applying all the selection criteria as described in §3, the number of W + jet events which survive is 37 and hence the estimated number of $Z \to \nu\nu$ + jet events in the above method is 63 ± 10. This is in very good agreement with our results from the simulated $Z \to \nu\nu$ + jets, i.e., 64 ± 7 and thus proves the credibility of the method discussed above.

8.2 *Estimation of W + jet event rate*

The $W \to \ell\nu$ + jet events mimic signal events when the charged lepton from W does not get detected. For muonic decay mode, when the muon is outside the detector acceptance region or if the muon is within acceptance region but the transverse momentum of the muon is less then the detection threshold value, the event is a potential background. For electron, though, the corresponding values of pseudorapidity and momentum thresholds are different as discussed before.

For estimating $W \to \mu\nu$ + jet background rate where the muon escapes detection, $W \to \mu\nu$ + jet events can be used where the muon is well-detected by utilizing shape analysis. In this method the number of selected events can be corrected to get the expected number of background events by taking into account the detector acceptance efficiency and isolation efficiency. However, these correction factors strongly depend on the muon momentum and hence two non-overlapping ranges have been considered: 5 GeV/c $< p_{\mathrm{T}} <$ 20 GeV/c and $p_{\mathrm{T}} >$ 20 GeV/c. The corresponding efficiencies are $\epsilon_1 = 5.94\%$ and $\epsilon_2 = 42\%$.

The total efficiency is thus given as $\epsilon = \epsilon_1 + \epsilon_2 = 47.94\%$ resulting in the correction factor of 1.08. Since we have 37 W + jet events which survive after all cuts, the corrected number of expected background event is about 40±7. This can be compared with our result of 43±7 events of type $W \to \mu\nu$ + jets obtained from cut-based analysis. Hence this method also can be considered robust for background estimation.

8.3 *Estimation of QCD multijets and inclusive $t\bar{t}$ processes*

The combined contribution of QCD and $t\bar{t}$ + jet events to the total background in the final selected sample can be estimated, simultaneously, using the so-called Matrix method. This method requires two uncorrelated variables which discriminate between signal and background processes. The most suitable combination is found to be the NV variable and the di-jet invariant mass M_{jj}, discussed in §5. The independence of these two variables can be checked by comparing the shape of NV variable for different M_{jj} cut values as shown in figure 8 (left). We can define four regions in NV vs. M_{jj} plane as shown in figure 8 (right). They are defined as A: NV < 4, $M_{jj} < 1200$ GeV/c^2, B: NV < 4, $M_{jj} > 1200$ GeV/c^2, C: NV > 4, $M_{jj} < 1200$ GeV/c^2 and D: NV > 4, $M_{jj} > 1200$ GeV/c^2. Thus region D corresponds to the signal selection region.

All the four regions have varying contributions from both signal and background events. Experimentally, the total contribution in each region is measured as

$$N_{\mathrm{T}}^{\mathrm{A}} = N_b^{\mathrm{A}} + N_s^{\mathrm{A}}, \quad N_{\mathrm{T}}^{\mathrm{B}} = N_b^{\mathrm{B}} + N_s^{\mathrm{B}},$$

$$N_{\mathrm{T}}^{\mathrm{C}} = N_b^{\mathrm{C}} + N_s^{\mathrm{C}}, \quad N_{\mathrm{T}}^{\mathrm{D}} = N_b^{\mathrm{D}} + N_s^{\mathrm{D}}.$$

If $\epsilon_{\mathrm{NV}}, \epsilon_{M_{jj}}$ are the efficiencies for NV and M_{jj} criteria, the number of events in four different regions can be given as

$$N^{\mathrm{A}} = (1 - \epsilon_{\mathrm{NV}}) \cdot (1 - \epsilon_{M_{jj}}), \quad N^{\mathrm{B}} = (1 - \epsilon_{\mathrm{NV}}) \cdot \epsilon_{M_{jj}},$$

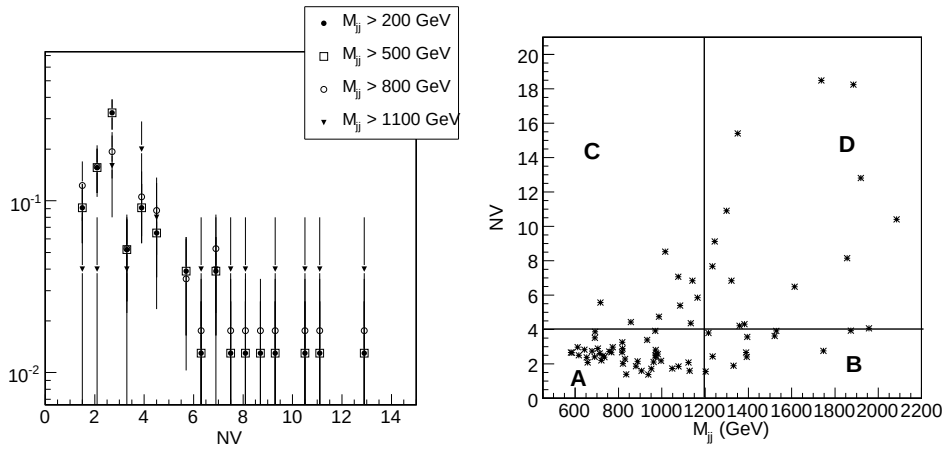

Figure 8. Comparison of NV shapes for different M_{jj} cut values for QCD background in $\hat{p}_t$ bin 50–70 GeV/c (left). Only the probability distribution is shown. It is clear that NV and M_{jj} are un-correlated to a very good extent. Right plot shows the scatter plot between M_{jj} and NV variable for $\hat{p}_t$ bin 50–70 GeV/c.

$$N^{\mathrm{C}} = \epsilon_{\mathrm{NV}} \cdot (1 - \epsilon_{M_{jj}}), \quad N^{\mathrm{D}} = \epsilon_{\mathrm{NV}} \cdot \epsilon_{M_{jj}}.$$

From Monte Carlo simulation of signal events, each N_s^i where i = A, B, C and D can be estimated accurately. After subtracting the signal contribution from regions A, B and C, the total background contribution in region D, N_b^{D}, due to all processes can be calculated assuming that the contribution of W + jet and Z + jet backgrounds in region D can be estimated by techniques discussed already. Hence the rates for QCD multijets and inclusive $t\bar{t}$ processes can be estimated by subtracting W + jet and Z + jet contributions in region D.

8.4 *Measurement of the efficiency for central jet veto criteria*

The efficiency of the central jet veto (CJV) condition for $W \to \mu\nu$ + jet, where the muon is not identified, can be measured by $W \to \mu\nu$ + jet events where the muon is identified and well measured. Similar efficiency for $Z \to \nu\nu$ + jet events can be estimated with $Z \to \mu\mu$ + jet events where the muons are identified and well measured. Additionally, the events must have at least two jets satisfying the off-line WBF conditions.

A sample of $W \to \mu\nu$ + jet event is considered where the event contains exactly one isolated muon of $p_{\mathrm{T}} > 20$ GeV/c, $|\eta| < 2.1$. The CJV efficiency is estimated to be 0.366 ± 0.02 which is in very good agreement with CJV efficiency already obtained from the analysis of MC sample for $W \to \mu\nu$ + jet events. The CJV efficiency for $Z \to \nu\nu$ + jet background is determined to be 0.346 ± 0.018 which again compares very well with the CJV efficiency estimated from simulated $W \to \mu\nu$ + jet events where the muon is not detected.

The CJV efficiency for $W \to e\nu$ + jet background events can be obtained by exactly the same method using $W \to e\nu$ + jet events where the electron is well reconstructed.

9. Conclusion

A strategy to search for the Higgs boson in CMS experiment in its invisible decay mode is investigated using weak boson fusion production mechanism at the LHC at the centre of mass energy of 14 TeV. The event topology and other kinematic properties of signal events are utilized to tackle various Standard Model background processes. Detailed simulation has been performed to account for detector and other experimental effects. A methodology for determining the signal significance has also been suggested. Different data-driven background estimation methods have been studied, which yield satisfactory results within statistical uncertainty. It is shown that an integrated luminosity of at least 10 fb^{-1} is needed to establish the presence of an invisibly decaying Higgs boson.

Acknowledgement

The authors would like to thank all of their collaborators in CMS experiment who have provided both direct and indirect support to carry out the study. S Bansal would like to thank CSIR-HRDG for funding.

References

[1] A S Joshipura and S D Rindani, *Phys. Rev. Lett.* **69(23)**, 3269 (1992)
[2] K Belotsky, D Fargion, M Khlopov, R Konoplich and K Shibaev, *Invisible Higgs boson decay into massive neutrinos of 4th generation*, hep-ph/0210153
[3] D Dominici, *Probing extra dimensions through the invisible Higgs decay*, hep-ph/0503216
[4] H C Cheng and J L Feng, *Phys. Rev. Lett.* **89(21)**, 211301
[5] F Boudjema, G Blanger and R M Godbole, *Invisible decays of the supersymmetric Higgs and dark matter*, hep-ph/0206311
[6] ALEPH, DELPHI, L3 and OPAL Collaborations: Searches for invisible Higgs bosons: Preliminary combined results using LEP data collected at energies up to 209 GeV, hep-ex/0107032v1, LHWG Note/2001-06
[7] S H Zhu, *Eur. Phys. J.* **C47**, 833 (2006)
[8] H Devoudiasl, T Han and H E Logan, *Phys. Rev.* **D71**, 115007 (2005)
[9] CMS Collaboration: CMS Detector Performance and Software, Physics Techinal Design Report, Volume I, CERN/LHCC 2006-001
[10] O J P Éboli and D Zeppenfeld, *Phys. Lett.* **B495**, 147 (2000)
[11] T Sjostrand, S Mrenna and P Skand, *J. High Energy Phys.* **05**, 026 (2006)
[12] M L Mangano, M Moretti, F Piccinini, R Pittau and A Polosa, *J. High Energy Phys.* **07**, 001 (2003)
[13] S Frixione and B R Webber, The MC@NLO 3.3 event generator, hep-ph/0612272

[14] CMS Collaboration: Performance of jet algorithms, CMS PAS JME-07-003, 2007
[15] CMS Collaboration: Plans for jet energy corrections at CMS, CMS PAS JME-07-002, 2007
[16] CMS Collaboration: Missing ET performance, CMS PAS JME-07-001, 2007
[17] S Baffioni *et al*, *Eur. Phys. J.* **C49**, 1099 (2007)
[18] CMS Collaboration: CMS Physics: Technical design report, CERN-LHCC-2006-001
[19] CMS Collaboration: Measurement of W and Z cross sections with electrons, CMS PAS EWK-07-001, 2007.
[20] CMS Collaboration, Measurement of W and Z cross sections with muons, CMS PAS EWK-07-002, 2007.
[21] CMS Collaboration: CMS High Level Trigger, CERN/LHCC 2007-021, LHCC-G-134, 29th June 2007
[22] S Bityukov, N Krasnikov and A Nikitenko, *On the combining significance*, arXiv:physics/0612178